

Si-doped $\text{Al}_x\text{Ga}_{1-x}\text{N}$ ($0.56 \leq x \leq 1$) layers grown by molecular beam epitaxy with ammonia

B. Borisov and V. Kuryatkov

Department of Electrical and Computer Engineering, Texas Tech University, Lubbock, Texas 79401

Yu. Kudryavtsev and R. Asomoza

SIMS laboratory of SEES, Department of Electrical Engineering, CINVESTAV, Mexico D.F. 07300, Mexico

S. Nikishin,^{a)} D. Y. Song, M. Holtz, and H. Temkin

Nano Tech Center, Texas Tech University, Lubbock, Texas 79401

(Received 15 June 2005; accepted 4 August 2005; published online 21 September 2005)

We describe experiments on Si doping in $\text{Al}_x\text{Ga}_{1-x}\text{N}$ grown by gas source molecular beam epitaxy with ammonia and silane. Growth conditions that minimize self-compensation were used to assure Si incorporation at a level of $2 \times 10^{20} \text{ cm}^{-3}$ for the entire range of compositions investigated, from $x=0.56$ to 1.0. These conditions resulted in donor concentrations of $\sim 1 \times 10^{19} \text{ cm}^{-3}$ up to $x=0.85$. Layers of $\text{Al}_x\text{Ga}_{1-x}\text{N}$ up to $x=0.85$ show good mobility and low resistivity. In these layers, the activation energy, E_a , of Si stays below $\sim 25 \text{ meV}$ and Si can be considered a shallow donor. For AlN content above $x=0.85$ the donor activation energy increases to $E_a \sim 250 \text{ meV}$ in AlN. The change in donor activation energy correlates with increased incorporation of oxygen and carbon.

© 2005 American Institute of Physics. [DOI: 10.1063/1.2061856]

There has been considerable recent progress in preparing conducting $n\text{-Al}_x\text{Ga}_{1-x}\text{N}$ doped with Si donors.¹⁻⁹ The donor efficiency is believed to decrease for high AlN content^{1-3,6-14} and the donor behavior appears particularly complex in AlN itself.^{6-9,15} A number of mechanisms have been proposed to explain this dependence. These include increased concentration of aluminum vacancies V_{Al} or formation of V_{Al} -oxygen complexes in AlN rich alloys¹³ and increased silicon self-compensation for high AlN content and high Si concentrations.¹⁴ The activation energy of Si was also found to increase with increased AlN content but neither the detailed dependence on the AlN fraction nor the mechanism responsible are understood.

This letter describes a systematic study of Si doping in $\text{Al}_x\text{Ga}_{1-x}\text{N}$ as a function of AlN content, for $0.56 \leq x \leq 1$. The samples were grown by gas source molecular beam epitaxy with ammonia on (0001) sapphire substrates using silane as a source of Si.⁴ Previous studies used metalorganic vapor phase epitaxy,^{1,2,5-7,10,12-14} also with silane, and plasma-assisted molecular beam epitaxy MBE^{3,8,9,11,15} using solid Si.

Epitaxial growth starts with the substrate nitridation at 900 °C. A 40-nm-thick layer of AlN is grown first at the same temperature to produce a two-dimensional (2D) Al-polar surface.¹⁶ Layers of silicon doped $\text{Al}_x\text{Ga}_{1-x}\text{N}$ with composition in the range of $0.56 \leq x \leq 1$ are grown next at 830 °C. The AlGa_N layers, with a thickness of $\sim 0.8 \mu\text{m}$, are grown under 2D conditions, as confirmed by *in situ* reflection high energy electron diffraction. Growth rates are calibrated using *in situ* spectroscopic pyrometry.¹⁷ The growth rate of $\sim 0.35 \mu\text{m/h}$ and the substrate temperature of 830 °C were kept constant for samples with different compositions. The ammonia flux was kept at $\sim 17 \text{ sccm}$, yielding the V/III ratio close to unity which is the boundary between Ga-rich

and N-rich conditions. These conditions, optimized for the growth of $\text{Al}_{0.75}\text{Ga}_{0.25}\text{N}$, are believed to result in efficient incorporation of Si into the group III sublattice.¹⁸ However, no significant changes in the carrier density were observed in samples grown under slightly different fluxes of ammonia, between 10 and 30 sccm.

The composition of all samples was confirmed by x-ray diffraction and optical reflectivity measurements. Secondary ion mass spectroscopy (SIMS) was used to measure Si, C, and O concentrations. In $\text{Al}_x\text{Ga}_{1-x}\text{N}$ with $x < 0.95$, SIMS shows background level of less than 5×10^{17} and $1 \times 10^{18} \text{ cm}^{-3}$ for C and O, respectively. Electrical parameters were determined by Hall measurements, from 200 to 370 K, using cloverleaf samples with Ti/Al/Ti/Au ohmic contacts.

Figure 1(a) plots the carrier density as a function of beam equivalent pressure (BEP) of silane. The BEP was measured with a Bayard-Alpert gauge placed at the substrate position. Figure 1(b) plots the carrier density as a function of silicon concentration in the alloy, measured by SIMS. Both sets of measurements were done for samples of $\text{Al}_{0.60}\text{Ga}_{0.40}\text{N}$ and $\text{Al}_{0.86}\text{Ga}_{0.14}\text{N}$. The carrier density, in both plots and for both alloy compositions, shows a clear maximum near the BEP of 8×10^{-9} – 10^{-8} Torr and the corresponding Si concentration of $(1-2) \times 10^{20} \text{ cm}^{-3}$. In this region, labeled II in Fig. 1, carrier densities reach $2 \times 10^{19} \text{ cm}^{-3}$ in $\text{Al}_{0.60}\text{Ga}_{0.40}\text{N}$ and $7 \times 10^{18} \text{ cm}^{-3}$ in $\text{Al}_{0.86}\text{Ga}_{0.14}\text{N}$. While quantitative comparisons between the plots of Figs. 1(a) and 1(b) are difficult to make, the general dependence of the carrier density is similar. Lower BEPs, region I, result in lower carrier densities and lower Si incorporation. In this region the carrier density can be controlled by adjusting the BEP of Si. On the other hand, higher BEPs of Si, in region III, result in decreased carrier densities, for samples of both compositions, demonstrating the importance of self-compensation of Si. At the maximum Si concentration of $7 \times 10^{20} \text{ cm}^{-3}$ the carrier density is limited to $\sim 3 \times 10^{17} \text{ cm}^{-3}$.

^{a)} Author to whom correspondence should be addressed; electronic mail: sergey.a.nikishin@ttu.edu

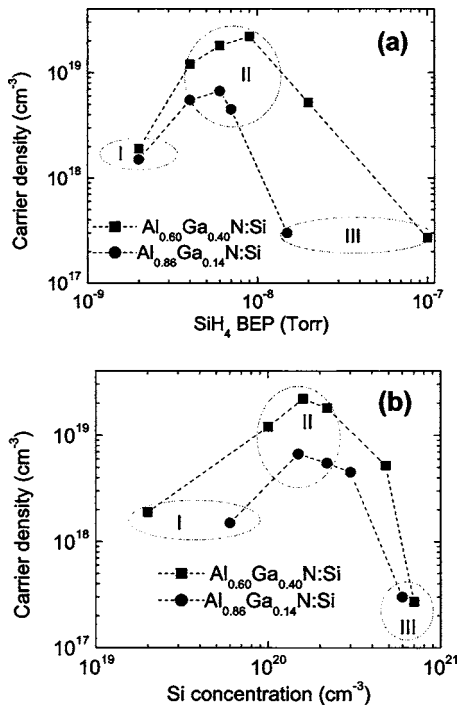


FIG. 1. The carrier density vs silane flux (a) and Si concentration (b).

The dependence of the carrier density on the alloy composition is plotted in Fig. 2(a). For samples grown under the same conditions of temperature, growth rate, III/V ratio, and the BEP of silane, the carrier concentration remains fairly constant, at $\sim 10^{19}$ cm⁻³, up to the AlN content of $x = 0.85$ – 0.88 . Under the growth conditions used here the carrier concentration decreases rapidly for higher AlN content. Similar trends have been observed previously,^{1–3,10–14} with some important differences. For instance, Kasu, and

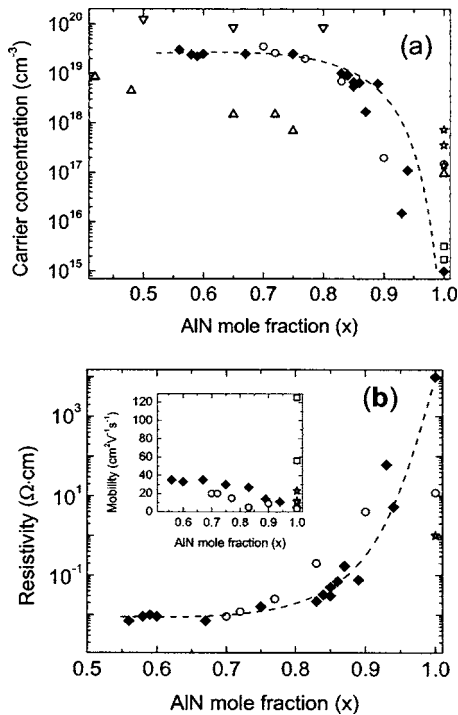


FIG. 2. Carrier density (a) and resistivity of Si doped AlGaIn vs AlN content measured in Hall experiments. ∇ — (Ref. 2), \triangle — (Ref. 3), \circ — (Ref. 6), \square — (Ref. 7), \star — (Ref. 8), \blacklozenge — this work.

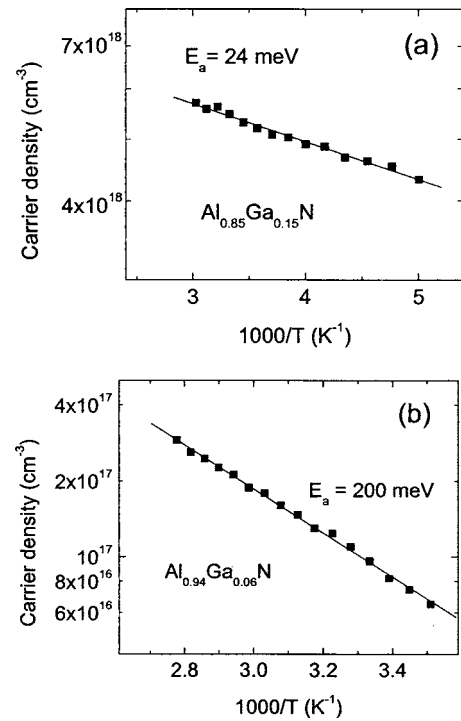


FIG. 3. Temperature dependence of carrier concentration in AlGaIn.

Kobayashi² and Nakarmi *et al.*⁶ observed a more gradual decrease in the carrier concentration with the AlN content. Furthermore, there are a number of different results for AlN, with carrier concentrations ranging from $\sim 10^{15}$ cm⁻³ (Ref. 7) to a high of 7×10^{17} cm⁻³ (Ref. 8) in samples grown under different conditions, as illustrated in Fig. 2(a). Resistivity of our Al_xGa_{1-x}N samples is plotted as a function of the AlN content in Fig. 2(b). These data are complementary to the carrier concentration dependence plotted in Fig. 2(a). Very low resistivities, on the order of 0.01 Ω cm, are obtained for AlN content up to $x = 0.75$. Resistivity increases by about an order of magnitude when the AlN content reaches $x = 0.9$. Between 0.9 and 1 we observe an exponential increase in resistivity. The inset of Fig. 2(b) plots the room temperature electron mobility dependence on composition. In our samples, mobility decreases from 40 cm²/V s in Al_{0.6}Ga_{0.4}N to ~ 5 cm²/V s in AlN, consistent with the resistivity data and increasing Si self-compensation.

Temperature dependent measurements of the Hall carrier density were used to extract the donor activation energy E_a . The experimental results are shown in Fig. 3 for two samples. The activation energy of 24 meV was measured in a sample of Al_{0.85}Ga_{0.15}N. Samples with lower AlN content show slightly lower activation energies, ~ 20 meV. The temperature dependence of the carrier concentration is, however, quite different in samples with higher content of AlN as shown in Fig. 3(b) for a sample of Al_{0.94}Ga_{0.06}N. The fit to the data was obtained from the expression taking into account acceptor compensation

$$\frac{n(n + N_A)}{N_D - N_A - n} = \frac{N_C}{2} \exp(-E_a/kT),$$

where n is the electron density, N_D is the donor concentration in the solid, N_A is the compensating acceptor concentration, and N_C is the density of states in the conduction band. The donor degeneracy factor is assumed to be two.² N_D , N_A , and

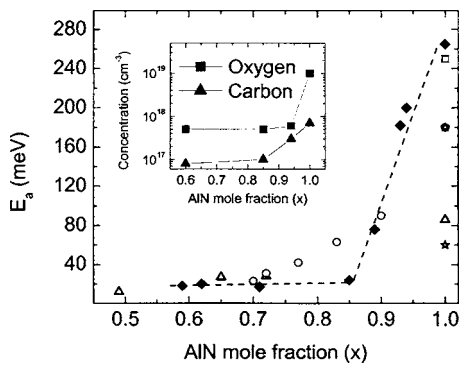


FIG. 4. Donor, Si, activation energy vs AlN content calculated from the temperature dependence of the carrier density. \triangle — (Ref. 3), \circ — (Ref. 6), \square — (Ref. 7), \star — (Ref. 8), \blacklozenge — this work. The inset shows oxygen and carbon concentration vs AlN content.

E_a are used as fitting parameters with a calculated value of $N_C = 3.3 \times 10^{18} \text{ cm}^{-3}$, obtained assuming an interpolated $m^* = 0.4 m_0$.¹⁹ The best fit to the data of Fig. 3(b) is obtained for $E_a = 200 \text{ meV}$, $N_D = 1.3 \times 10^{20} \text{ cm}^{-3}$, and $N_A = 7 \times 10^{17} \text{ cm}^{-3}$. This should be compared to the silicon concentration of $1.6 \times 10^{20} \text{ cm}^{-3}$ and the oxygen and carbon concentrations of 6×10^{17} and $2 \times 10^{17} \text{ cm}^{-3}$, respectively, determined by SIMS measurements. A simple exponential fit to the data of Fig. 3(b) yields $E_a = 183 \text{ meV}$.

The donor activation energies are summarized as a function of composition in Fig. 4. The E_a is fairly constant in our samples up to $\text{Al}_{0.85}\text{Ga}_{0.15}\text{N}$ and Si remains a shallow donor. This is somewhat different from previous results,⁶ obtained through the temperature dependence of resistivity, which showed a gradual increase in E_a as a function of the alloy composition. In samples closer to AlN the activation energy increases rapidly. The results obtained here for AlN are in good agreement with some of the recent measurements reporting $E_a \sim 250 \text{ meV}$.⁷ However, in AlN the activation energy is strongly dependent on the growth conditions as discussed recently by Hermann *et al.*⁹

The increase in E_a in $\text{Al}_x\text{Ga}_{1-x}\text{N}$ with $x > 0.85$ correlates with increased incorporation of oxygen and carbon seen in SIMS measurements as shown in the inset of Fig. 4. For instance, the carbon level is independent of the AlN content up to $x = 0.85$, at $1 \times 10^{17} \text{ cm}^{-3}$, but increases up to $6 \times 10^{17} \text{ cm}^{-3}$ for $x = 1$. Similarly, the oxygen concentration goes up from $6 \times 10^{17} \text{ cm}^{-3}$ for $x < 0.85$ to $1 \times 10^{19} \text{ cm}^{-3}$ for $x = 1$. Both oxygen and carbon are electrically active in Al-GaN. Oxygen is believed to be involved in formation of DX centers¹³ and carbon may act as an acceptor in AlN.²⁰ However, the absolute levels of these impurities are quite low even in AlN and they could influence E_a only by formation of defect complexes. The reason for the increased incorporation of compensating impurities for $x > 0.85$ is not known. We can only speculate that impurities such as CO or CO_2 that may be present in trace concentrations in ammonia are cracked more efficiently at Al-rich surfaces, similar to the behavior of ammonia itself. The incorporation of these compensating impurities can be controlled by changes in growth conditions such as the growth rate and the V/III ratio and by

purification of ammonia. These effects should be considered in models of Si incorporation in Al-rich AlGaN.

In summary, we carried out experiments of Si doping in $\text{Al}_x\text{Ga}_{1-x}\text{N}$ grown with ammonia and silane. Under growth conditions that minimize self-compensation and result in incorporation of Si at a concentration of $2 \times 10^{20} \text{ cm}^{-3}$, carrier concentrations of $\sim 1 \times 10^{19} \text{ cm}^{-3}$ can be obtained up to $x = 0.85$. These layers of $\text{Al}_x\text{Ga}_{1-x}\text{N}$ show good mobility and low resistivity. In these layers, Si is a well behaved shallow donor with $E_a \sim 20 \text{ meV}$. For AlN content above $x = 0.85$ the donor activation energy increases to $E_a \sim 250 \text{ meV}$ in AlN. The change in donor activation energy correlates with increased incorporation of oxygen and carbon.

This study was supported by NSF (ECS-0323640 and ECS-0304224), DARPA under the SUVOS program monitored by Dr. J. Carrano, and the J. F. Maddox Foundation.

- ¹K. B. Nam, J. Li, M. L. Nakarmi, J. Y. Lin, and H. X. Jiang, Appl. Phys. Lett. **81**, 1038 (2002).
- ²Y. Taniyasu, M. Kasu, and N. Kobayashi, Appl. Phys. Lett. **81**, 1255 (2002).
- ³J. Hwang, W. J. Schaff, L. Eastman, S. T. Bradley, L. J. Brillson, D. C. Look, J. Wu, W. Walukiewicz, M. Furis, and A. N. Cartwright, Appl. Phys. Lett. **81**, 5192 (2002).
- ⁴G. Kipshidze, V. Kuryatkov, B. Borisov, S. Nikishin, M. Holtz, S. N. G. Chu, and H. Temkin, Phys. Status Solidi A **192**, 286 (2002).
- ⁵P. Cantu, S. Keller, U. K. Mishra, and S. P. DenBaars, Appl. Phys. Lett. **82**, 3683 (2003).
- ⁶M. L. Nakarmi, K. H. Kim, K. Zhu, J. Y. Lin, and H. X. Jiang, Appl. Phys. Lett. **85**, 3769 (2004).
- ⁷Y. Taniyasu, M. Kasu, and N. Kobayashi, Appl. Phys. Lett. **85**, 4672 (2004).
- ⁸T. Ive, O. Brandt, H. Kostial, K. J. Friedland, L. Däweritz, and K. H. Ploog, Appl. Phys. Lett. **86**, 024106 (2005).
- ⁹M. Hermann, F. Furtmayr, A. Bergmaier, G. Dollinger, M. Stutzmann, and M. Eickhoff, Appl. Phys. Lett. **86**, 192108 (2005).
- ¹⁰M. D. Brenser, W. G. Perry, T. Zheleva, N. V. Edwards, O. H. Nam, N. Parikh, D. E. Aspnes, and R. F. Davis, MRS Internet J. Nitride Semicond. Res. **1**, 8 (1996).
- ¹¹D. Korakakis, H. M. Ng, K. F. Ludwig, Jr., and T. D. Moustakas, Mater. Res. Soc. Symp. Proc. **449**, 233 (1997).
- ¹²A. Y. Polyakov, N. B. Smirnov, A. V. Govorkov, M. G. Mil'vidskii, J. M. Redwing, M. Shin, M. Skowronski, D. W. Greve, and R. G. Wilson, Solid-State Electron. **42**, 627 (1998).
- ¹³M. D. McCluskey, N. M. Jonson, C. G. Van de Walle, D. P. Bour, M. Kneissl, and W. Walukiewicz, Phys. Rev. Lett. **80**, 4008 (1998).
- ¹⁴M. C. Wagener, G. R. James, and F. Omnès, Appl. Phys. Lett. **83**, 4193 (2003).
- ¹⁵R. Zeisel, M. W. Bayerl, S. T. B. Goennenwein, R. Dimitrov, O. Ambacher, M. S. Brand, and M. Stutzmann, Phys. Rev. B **61**, R16283 (2000).
- ¹⁶G. Kipshidze, V. Kuryatkov, K. Choi, İ. Gherasoiu, B. Borisov, S. Nikishin, M. Holtz, D. Tsvetkov, V. Dmitriev, and H. Temkin, Phys. Status Solidi A **188**, 881 (2001).
- ¹⁷S. A. Nikishin, S. Francoeur, and H. Temkin, Mater. Res. Soc. Symp. Proc. **639**, G.6.57.1 (2001).
- ¹⁸S. Nikishin, G. Kipshidze, V. Kuryatkov, K. Choi, İ. Gherasoiu, L. Grave de Peralta, A. Zubrilov, V. Tretyakov, K. Copeland, T. Prokofyeva, M. Holtz, R. Asomoza, Yu. Kudryavtsev, and H. Temkin, J. Vac. Sci. Technol. B **19**, 1409 (2001).
- ¹⁹*Properties of Advanced Semiconductor Materials: GaN, AlN, InN, SiC, SiGe*, edited by M. E. Levinstein, S. L. Rumyantsev, and M. S. Shur (Wiley, New York, 2001).
- ²⁰H. Katayama-Yoshida, R. Kato, and T. Yamamoto, J. Cryst. Growth **231**, 428 (2001).